Crossover between ordinary and normal transitions in two dimensional critical Ising films

A. Maciołek,[1,2] A. Ciach,[2] and A. Drzewiński[3]
[1]*H. H. Wills Physics Laboratory, University of Bristol, Bristol BS8 1TL, United Kingdom*
[2]*Institute of Physical Chemistry, Polish Academy of Sciences, Department III, Kasprzaka 44/52, PL-01-224 Warsaw, Poland*
[3]*Institute of Low Temperature and Structure Research, Polish Academy of Sciences, P.O. Box 1410, Wrocław 2, Poland*
(Received 19 January 1999)

We investigate two dimensional critical Ising films of width L with surface fields $H_1=H_L$ in the crossover between ordinary ($H_1=0$) and normal ($H_1=\infty$) transitions. Using exact transfer-matrix diagonalization and density matrix renormalization-group (DMRG) methods, we calculate magnetization profiles $m(z)$, the excess magnetization Γ, and the analog of the solvation force $f_{\rm solv}$ as functions of H_1 for several L. Scaling functions of the above quantities deviate substantially from their asymptotic forms at fixed points for a broad region of the scaling variable $LH_1^2 \sim L/l_1$, where l_1 is the length induced by the surface field H_1. The scaling function for $|f_{\rm solv}|$ has a deep minimum near $LH_1^2=1$, which is about one order of magnitude smaller than its value at both fixed points (the ''Casimir'' amplitude). For weak H_1 ($l_1>L$) the magnetization profile has a *maximum* at the center of the film, and $f_{\rm solv}$ decays much *faster* than L^{-2}. For stronger H_1 ($1<l_1<L$), the magnetization has *two maxima* at a distance $\sim l_1$ from the walls, and the solvation force decays much *slower* than L^{-2}. For $L \gg l_1$ the solvation force decays according to the universal power law $f_{\rm solv} \sim L^{-2}$. The results of the approximate DMRG method show remarkable agreement with the exact ones. [S1063-651X(99)00209-3]

PACS number(s): 64.60.Fr, 05.50.+q, 68.35.Rh

I. INTRODUCTION

It is now well established, both theoretically and experimentally, that the critical properties of systems such as magnets, binary alloys, fluid mixtures or simple fluids, are modified in the vicinity of a surface [1–3]. In general, each bulk universality class of critical phenomena splits into several surface universality classes depending on whether the tendency to order in the surface is enhanced or de-enhanced compared to the bulk. The leading critical behavior of the semi-infinite systems belonging to the particular surface universality class is described by the renormalization-group transformation fixed points of the surface enhancement of the interactions c, corresponding to the ordinary ($c=\infty$), special ($c=0$), and extraordinary ($c=-\infty$) transitions, all related to a vanishing surface external field H_1 (for example, the surface is exposed to a vacuum). In physical systems a surface external field is usually present—for instance, in fluids the walls of the container attract particles. A surface field explicitly breaks the symmetry at the surface, inducing ordering in the surface layer, and the corresponding surface universality class, the normal transition, is related to the infinitely strong surface field H_1 and to $c=\infty$ [4]. The shapes of the order parameter (OP) profiles are the same when the symmetry is explicitly or spontaneously broken at the surface, provided that the symmetry breaking fields are infinitely strong. Hence the normal and extraordinary transitions are equivalent.

In this work we restrict our attention to ordinary and normal transitions, and the crossover between them. This case corresponds, for example, to fluids or binary fluid mixtures in contact with various surfaces (various H_1) and to the semi-infinite Ising systems. Sufficiently close to the critical point the physical quantities are described by scaling functions. If the length scale is set to the bulk correlation length ξ_b, then the scaling variable related to the surface can be chosen as $H_1 \tau^{-\Delta_1^{\rm ord}}$, where $\tau=(T-T_c)/T_c$, with T denoting temperature and T_c its critical value, and $\Delta_1^{\rm ord}$ is the surface critical exponent [2]. For $\tau \to 0$ the scaling variable tends to its fixed point value, and the scaling functions assume asymptotic forms corresponding to the respective fixed point [4]. The scaling variable $H_1 \tau^{-\Delta_1^{\rm ord}}$, taken to an appropriate power, represents the ratio between ξ_b and the length $l_1 = H_1^{-\nu/\Delta_1^{\rm ord}}$ induced by the surface field H_1 (ν has its standard meaning). The asymptotic critical region of each surface universality class corresponds to this ratio going to ∞ or 0. For a mesoscopic or macroscopic ξ_b this means physically that l_1 is either microscopic or macroscopic but orders of magnitude larger than the bulk correlation length, respectively, and changing the surface field H_1 is irrelevant for the behavior of the studied quantities. This is the physical reason for the universality. Accordingly, there have been numerous theoretical efforts to investigate the individual surface universality classes. However, experiments are generically not carried out at the fixed points, and for systems with weak H_1 the length l_1 can be one or two orders of magnitude larger than the molecular size. On a mesoscopic length scale the OP may depend on whether the distance from the surface z is smaller, comparable to or larger than l_1. The shape of the OP can influence other physical quantities. Thus in the regime of $l_1/\xi_b = O(1)$ the behavior of the critical system is no longer universal in the sense that it depends on the strength of H_1 and so developing a detailed understanding of the crossover region between the fixed points is important.

Recently, for semi-infinite Ising-like systems in the crossover between the ordinary and the normal transitions, it was found that the OP profile is a nonmonotonic function of the distance from the surface z. Close to the surface $m(z)$ *increases*, and only for $z>l_1$ the universal ''normal'' fixed point behavior, i.e., a decaying OP, occurs [5,6]. Moreover,

it was pointed out that for $\xi_b \sim l_1$ (a weak surface field H_1) the amount of the adsorbed order as a function of τ is described by the power law $\tau^{\beta-\Delta_1^{\mathrm{ord}}}$ [7]. This prediction agrees very well with the recent experiments of Ref. [8]. Only much closer to the critical point ($\xi_b \gg l_1$) does a crossover to the universal power law $\tau^{\beta-\nu}$ take place. This particular behavior is related to the role played by the length l_1 which has been given a physical interpretation as an approximate distance from the surface up to which the OP responds linearly to H_1 [7].

Motivated by the above results, we ask how the presence of weak surface magnetic fields influences the behavior of the *confined* system near bulk criticality. In confined systems the relevant length scales, i.e., the width of the film, L, and l_1, can be comparable to each other and much smaller than ξ_b, corresponding to the universal, asymptotic critical behavior which takes place when $\xi_b \gg l_1$. In films of a mesoscopic width L the OP should depend sensitively on whether L is larger than, comparable to, or smaller than l_1. To verify this prediction we study the behavior of two dimensional (2D) Ising films as a function of the surface magnetic field H_1. We concentrate on the competition between the length scale l_1 and the width of the film, L, *at* bulk criticality. We investigate the shape of the magnetization profile and the excess magnetization (adsorption) Γ, which, for fluids, can be measured directly by volumetric measurements. Previously these quantities were studied in Ising films only for strong surface fields acting on the first, H_1, and the Lth, H_L, layers, i.e., $H_1, H_L = \pm\infty$, corresponding to the fixed points.

An important thermodynamic quantity for a confined system is the solvation force, sometimes called the disjoining pressure [9]. For a fluid this is the excess pressure (over the bulk value fixed by the reservoir) arising from confinement, and can be measured directly by the surface force apparatus or atomic force microscopes [10]. In the critical confined systems this force becomes long ranged as a result of critical fluctuations, a phenomenon which is a direct analog of the well-known Casimir effect in electromagnetism [11,12]. Contrary to the usual dispersion forces, this force is governed by *universal scaling functions*. At fixed points these scaling functions reduce to the universal Casimir amplitudes. In recent years this so-called ''critical Casimir effect'' has attracted increasing theoretical interest, and many results are now available [12–18]. All of them are for $H_1, H_L = 0$ or $\pm\infty$. To our knowledge, the scaling function in the crossover regime between the ordinary and normal transition has not been studied. Comparing Casimir amplitudes for $d=2$ Ising films [see Eqs. (2.24) and (2.25) below], which are known exactly for $H_1 = H_L = 0$ and $H_1 = H_L = \pm\infty$ [13,17] one could come to the conclusion that the scaling function might be almost independent of the value of H_1 between these fixed points, because Casimir amplitudes at these extreme values of the surface fields take the same value equal to $-\pi/48$. Our expectation is that when the length scale l_1 becomes comparable with the width of the film, a nontrivial dependence of the scaling function on H_1 should occur.

We perform calculations using two methods: exact transfer-matrix diagonalization and the density matrix renormalization-group (DMRG) method [19]. The DMRG method was successfully employed for a series of two dimensional classical systems for which no exact solutions are available [20–23]. By implementing the exact diagonalization of the transfer matrix for 2D Ising films with arbitrary surface fields, we are able to test more systematically the accuracy of the DMRG method, especially for the largest widths $L \approx 200$. This test is important as we would like to use the DMRG method to study 2D Ising films away from the critical point including the case of nonzero bulk field.

The layout of the paper is as follows: in Sec. II we define the model, and give a survey of the most relevant results from the theory of critical phenomena for semi-infinite and finite systems in a slitlike geometry. In the subsequent sections we report our results. Section III analyzes the behavior of the magnetization profiles and the adsorption Γ at bulk criticality. The scaling functions for magnetization profiles and Γ are presented and discussed. The accuracy of the magnetization profiles from the DMRG method is discussed. Results for the solvation force at the bulk critical temperature T_c are presented in Sec. IV. The accuracy of the free energy from the DMRG method is discussed and the scaling function of the solvation force is also shown and discussed. Section V summarizes our work and states our conclusions.

II. THEORY

We consider the 2D Ising film defined on the square lattice $L \times M$, $M \to \infty$. The lattice consists of L rows at spacing $a \equiv 1$, so that the width of the film is $La = L$. At each site, labeled $i, j, \ldots$, there is an Ising spin variable taking the value $\sigma_i = \pm 1$. We assume nearest-neighbor interactions of strength J, and a Hamiltonian of the form

$$\mathcal{H} = -J\left[\sum_{\langle i,j\rangle} \sigma_i\sigma_j - H_1\sum_i^{(1)} \sigma_i - H_L\sum_i^{(L)} \sigma_i\right], \qquad (2.1)$$

where the first sum runs over all nearest-neighbor pairs of sites, while the last two sums run, respectively, over the first and the Lth rows. H_1 and H_L are the surface fields corresponding to direct, short range (''contact'') interactions between the walls and the spins in the film. H_1 and H_L are both measured in units of J. We assume that $H_1 = H_L > 0$.

For the 2D Ising model in semi-infinite geometry there exist two surface universality classes, since the boundary is one dimensional. There is only one relevant scaling field pertaining to the surface, the surface magnetic field H_1 [2]. The two universality classes are $H_1 = 0$, the ordinary transition, and $H_1 = \infty$, the normal transition, representing unstable and stable fixed points of the renormalization-group flow, respectively [1,2].

A. Semi-infinite systems

The scaling law for the OP profile in the vicinity of the surface which favors one of the phases was given by Fisher and de Gennes [24]. In the critical regime, $|\tau| \ll 1$, the magnetization and the excess magnetization (adsorption) Γ have the scaling forms:

$$m(z) = \tau^{\beta}\mathcal{M}_0\left(\frac{z}{\xi_b}, y\right), \qquad (2.2)$$

$$\Gamma \equiv \int_0^\infty m(z)dr = \tau^\beta \xi_b \mathcal{G}_0(y), \tag{2.3}$$

where z is the distance measured normal to the surface, located at $z=0$. β is the critical exponent describing the vanishing of the bulk (OP) magnetization. These formulas refer to $\tau>0$ and the bulk magnetic field $H=0$. $\mathcal{M}_0$ and $\mathcal{G}_0$ are universal scaling functions of the variable

$$y = \tau^{-\nu} H_1^{\nu/\Delta_1} \sim \xi_b / l_1 \tag{2.4}$$

and $l_1 = A_{l_1} H_1^{-\nu/\Delta_1}$. $\Delta_1 \equiv \Delta_1^{\rm ord}$ is the surface gap exponent. For the 2D Ising model $\Delta_1 = 1/2$, and there exists analytical expression for l_1 [25]; thus we can calculate the amplitude A_{l_1}: $A_{l_1} \approx 0.909(1)$.

At the critical point and $H_1=0$ (ordinary transition) the magnetization profile is zero for any distance $z \geqslant 0$ from the surface, and accordingly $\Gamma=0$. For $H_1=\infty$ (normal transition) $m(z)$ starts from $m_1=1$ at the surface and then decays to the bulk equilibrium value. At the critical point the OP profile takes the critical-point scaling form

$$m(z,H_1,T_c) \sim z^{-\beta/\nu} \mathcal{M}_{0c}(z/l_1), \tag{2.5}$$

with $\mathcal{M}_{0c}(\zeta)$ approaching a constant for $\zeta \to \infty$. Hence, at the critical point,

$$m(z,H_1 \to \infty, T_c) \sim z^{-\beta/\nu} \tag{2.6}$$

for distances $z \gg l_1$. In the 2D Ising model $\beta/\nu = 1/8$. For $T \neq T_c$ a crossover to the exponential decay $\sim \exp(-z/\xi_b)$ takes place at a distance $z \sim \xi_b$ from the surface. For y tending to the fixed point $y=\infty$, $\mathcal{G}_0(y) \approx$ const, and Γ diverges for $\tau \to 0$ according to the universal power law

$$\Gamma \sim \tau^{\beta-\nu}. \tag{2.7}$$

In the *crossover* region between $H_1=0$ and $H_1=\infty$, the OP profile steeply increases close to the surface to values $m(z) \gg m_1$ [5,6,26] and this is contrary to the mean-field (MF) expectation. At bulk criticality this growth occurs for $z < l_1$.

In the 2D Ising model the magnetization scaling function behaves in the following way at the critical point [27]:

$$\mathcal{M}_{0c} \sim \zeta^{y_1} \ln \zeta \quad \text{for} \quad \zeta \ll 1, \tag{2.8}$$

with $y_1 = \Delta_1^{\rm ord}/\nu = (d-\eta_\parallel)/2 = 1/2$, where $\eta_\parallel$ is the anomalous dimension governing the decay of the correlations in the direction parallel to the surface [2]. Hence, for $z \ll l_1$, the magnetization is described by

$$m(z,H_1,T_c) \sim H_1 z^\kappa \ln(H_1 z), \tag{2.9}$$

where κ for the 2D Ising model is $\kappa = (\Delta_1^{\rm ord} - \beta)/\nu = 1 - \eta_\perp = 3/8$. For a given value of H_1 the magnetization $m(z)$ grows as $\sim z^{3/8} \ln z$ for $z \leqslant l_1$. For $z \sim l_1$ the profile has a maximum, and for $z > l_1$ the decay of the OP profile is characteristic of that for the normal transition, i.e., $m(z) \approx A z^{-\beta/\nu}$ with the amplitude A independent of H_1.

The (Monte Carlo) literature values for the 3D Ising model are $\beta/\nu = 0.518(7)$ [28] and $y_1 \approx 0.73$. The latter was obtained by employing the scaling relation $y_1 + \beta_1^{\rm ord}/\nu = d - 1$ together with the Monte Carlo result $\beta_1^{\rm ord}/\nu \approx 1.27$ [5]. Hence for the 3D Ising model the growth of $m(z)$ for $z \ll l_1$ is described by a power law

$$m(z,H_1,T_c) \sim H_1 z^\kappa, \tag{2.10}$$

with $\kappa \approx 0.21$. In the MF approximation $\Delta_1^{\rm ord} = \beta = 1/2$, so that $\kappa = 0$. Thus, in this case one has $m(z \to 0) = m_1$ and a monotonically decaying OP profile consistent with behavior (2.10).

To understand this behavior note that at the ordinary transition the surface remains paramagnetic at $T=T_c$, and hence should respond linearly to a weak surface field H_1. The same should hold in the immediate neighborhood of a surface, thus

$$m(z) \sim m_1 \sim H_1 \quad \text{for} \quad z \to 0 \quad \text{and} \quad H_1 \to 0. \tag{2.11}$$

Equations (2.11) and (2.5) can be simultaneously satisfied if $\mathcal{M}_{0c} \sim \zeta^{\Delta_1/\nu}$, which leads to $m(z) \sim z^\kappa$.

The mechanism leading to the increase of the $m(z)$ for $z < l_1$ can be explained heuristically on the basis of the behavior of correlations in the near-surface region [6]. At $T = T_c$ the correlations decay algebraically. The decay in planes parallel to the surface is described by $r^{-d+2-\eta_s}$, where r is the distance within the plane parallel to the surface. The surface suppresses fluctuations, and the exponent η_s depends on the distance from it and on z/r. For $z < l_1$, that is in the near-surface region, η_s assumes its bulk value η (slow decay) if $r \ll z$ and for $r \gg z$, $\eta_s = \eta_\parallel^{\rm ord} > \eta$ (fast decay). The effective range of correlations $\xi_\parallel$ may be identified with the distance at which the crossover between the slow and fast decay occurs, $\xi_\parallel \sim z$. A weak surface field is equivalent to several boundary spins having a fixed (the same) orientation. The magnetization induced by these spins at the distance z from the surface is proportional to H_1, to the correlation function in the perpendicular direction, describing the decay of the order, $\langle m(0)m(z)\rangle \sim z^{-d+2-\eta_\perp^{\rm ord}}$, and to the correlated area in the plane parallel to the surface, $\xi_\parallel^{d-1}$, which can be influenced by a single surface spin. All these terms together give

$$m(z) \sim H_1 \langle m(0)m(z)\rangle \xi_\parallel^{d-1} \sim H_1 z^{1-\eta_\perp^{\rm ord}}, \tag{2.12}$$

valid for $z < l_1$. Scaling relations [6] give, in turn, $1 - \eta_\perp^{\rm ord} = \kappa$.

B. Finite-size scaling

For a film of finite width, $m(z)$ and Γ, defined as in Eq. (2.3) but with the upper limit of integration equal to L, should have the following forms [29]:

$$m(z,H_1,T,L) = \tau^\beta \mathcal{M}\left(\frac{z}{L}; x, y\right) \tag{2.13}$$

and

$$\Gamma = \tau^\beta L \mathcal{G}(x,y), \tag{2.14}$$

where $\mathcal{M}$ and $\mathcal{G}$ are scaling functions, y is defined in Eq. (2.4), and

$$x = L\tau^{\nu}. \tag{2.15}$$

With this choice of scaling variables, $x \sim L/\xi_b$ and $y \sim \xi_b/l_1$. At criticality the OP profile takes the scaling form [2]

$$m(z,H_1,T_c,L) = z^{-\beta/\nu}\mathcal{M}_c\left(\frac{z}{L};xy\right), \tag{2.16}$$

or, equivalently,

$$m(z,H_1,T_c,L) = L^{-\beta/\nu}\mathcal{N}_c\left(\frac{z}{L};xy\right), \tag{2.17}$$

where $\mathcal{M}_c$ and $\mathcal{N}_c$ are scaling functions, and $xy \sim L/l_1$ is a scaling variable appropriate for $T = T_c$. The adsorption Γ then has a form

$$\Gamma \sim L^{(\nu-\beta)/\nu}\mathcal{G}_c(xy), \tag{2.18}$$

where

$$\mathcal{G}_c(xy) = \int_0^1 d\zeta\,\zeta^{-\beta/\nu}\mathcal{M}_c(\zeta,xy). \tag{2.19}$$

The shapes of the scaling functions $\mathcal{N}_c$ and $\mathcal{G}_c$ for the 2D Ising film are known only at the fixed points $y = 0$ and $y = \infty$. The exact analytic prediction for the entire profile at $y = \infty$ was first given on the basis of conformal invariance [30], and then calculated from the exact transfer matrix solution [31]. It is

$$m(z,H_1,T_c,L) = \mathcal{A}[(L/\pi)\sin(\pi z/L)]^{-1/8}, \tag{2.20}$$

so that the scaling function is $\mathcal{N}_c(\zeta,\infty) = \mathcal{B}[\sin(\pi\zeta)]^{-1/8}$, where $\mathcal{A}$ and $\mathcal{B}$ are constants.

The behavior of Γ for $y \gg 1$ is given by Eq. (2.18) with $\mathcal{G}_c(xy)$ replaced by a constant, $\mathcal{G}_c(\infty)$, and in the limit of $y \to \infty$, $\Gamma \sim L^{(\nu-\beta)/\nu}$ with $(\nu-\beta)/\nu = 7/8$ for the 2D Ising system.

Until now the shape of the OP profiles, the adsorption Γ, and their scaling functions were not studied in full detail away from the fixed points. Some results for the OP profiles, obtained from Monte Carlo simulations of a 2D Ising film with weak surface fields, were presented in Ref. [27]. This work focused mainly on the analysis of the near-surface behavior of $m(z)$, and the entire profile was shown only for $H_1/k_BT = 0.01$ and for various temperatures below and above T_c. As far as the near-surface behavior is concerned, it was found that when $l_1 \ll L$ the z dependence of the magnetization profile near the surface is the same as in the semi-infinite systems, i.e., $m(z)$ grows as $z^{3/8}\ln z$ for $z < l_1$. The authors argue that the amplitude of Eq. (2.9) should be different from that in the semi-infinite system. This follows from the exact results for films (finite L), which show that the leading behavior of $m_1(H_1)$ as $H_1 \to 0$ is $m_1 \sim H_1 \ln L$ rather than $m_1 \sim H_1 \ln H_1$ for semi-infinite systems [32]. The L-dependent prefactor in front of Eq. (2.9) was visible in the results of the Ref. [27].

C. Solvation force

The free energy per site of the 2D Ising film with two surface fields $H_1 = H_L$ can be written as

$$f(L,T,H_1) = f_b + 2f_w/L + f^*(L)/L, \tag{2.21}$$

where f_b is the bulk free energy, f_w is the L-independent surface contribution from each wall, and f^* is the finite-size correction to the free energy. The latter vanishes for $L \to \infty$. Such a term gives rise to the generalized force, which is analogous to the solvation force between the plates in confined fluids [9]:

$$f_{\text{solv}} = -(\partial f^*/\partial L)_{H,T}. \tag{2.22}$$

On the basis of the scaling argument, Fisher and de Gennes [24] predicted that, when $T = T_c$ and the bulk field $H = 0$, f^* has the form

$$f^* = A_{1,L}k_BT_cL^{-(d-1)} \tag{2.23}$$

as $L \to \infty$. The constant $A_{1,L}$ depends on the choice of the surface fields. Later, Privman and Fisher [33] argued that the amplitude $A_{1,L}$ should depend *only* upon the relative signs of H_1 and H_L. The slow, algebraic decay predicted by Eq. (2.23) is associated with the bulk critical fluctuations and is analogous to the Casimir effect. For the 2D Ising film the amplitudes $A_{1,L}$ have been calculated exactly [13,17] for the following choice of the surface fields: $H_1 = H_L = \pm\infty, 0$ and $H_1 = -H_L = \pm\infty$. The leading-order decay for $L \to \infty$ of the solvation force at these fixed points is the following:

$$f_{\text{solv}}/k_BT_c = -\frac{\pi}{48}L^{-2}, \quad H_1 = H_L = \pm\infty, 0, \quad T = T_c, \tag{2.24}$$

$$f_{\text{solv}}/k_BT_c = \frac{23}{48}\pi L^{-2}, \quad H_1 = -H_L = \pm\infty, \quad T = T_c. \tag{2.25}$$

From the general theory of critical finite-size scaling [29] it follows that the solvation force for identical surface fields should take the following scaling form:

$$f_{\text{solv}} = L^{-d}\mathcal{F}(x,y). \tag{2.26}$$

At $T = T_c$ the scaling relation takes the critical form

$$f_{\text{solv}} = L^{-d}\mathcal{F}_c(xy). \tag{2.27}$$

Examining Eq. (2.27), we see that it does not follow that the critical amplitudes are sufficient to describe the solvation force in the whole range of the surface fields H_1, i.e., in the crossover between $xy = 0$ and $xy = \infty$. Only for $xy \to \infty$ or $xy \to 0$ does the scaling function reduce to the critical amplitudes.

For the 2D Ising model, where the critical exponent $\alpha = 0$ and the bulk free energy diverges logarithmically in τ as $T \to T_c$ [32], the appropriate form of the critical finite-size scaling of f_{solv} should also contain a logarithmic term

$$f_{\text{solv}} = L^{-2}\mathcal{F}_1(x,y) + L^{-2}\ln L\,\mathcal{F}_2(x,y) \tag{2.28}$$

where $\mathcal{F}_1$ and $\mathcal{F}_2$ are analytic functions of x and y. The scaling function for the solvation force was evaluated and analyzed in a wide range of variable x in Ref. [14], but only in the cases $H_1=H_L=\pm\infty$ and $H_1=-H_L=\pm\infty$.

III. RESULTS FOR MAGNETIZATION PROFILES AND ADSORPTION

The exact diagonalization of the transfer matrix for the 2D Ising film with arbitrary surface fields was performed by Maciołek and Stecki [34], and the exact formula for the average magnetization $m_l \equiv \langle \sigma_l \rangle$ across the film was given in Ref. [34]. We use this expression to calculate numerically, but to machine accuracy, the magnetization profiles at the bulk critical point, for different surface fields H_1.

The DMRG method for 2D classical systems is based on the transfer-matrix approach. It deals with $L\times\infty$ strip geometries for which it provides a very efficient algorithm for the construction of effective transfer matrices for large L. Typical numerical calculations for the standard transfer-matrix method in the Ising systems are restricted to strips of rather small widths ($L\leqslant 20$), whereas the DMRG method has enabled us to consider strips with a width up to $L=200$.

In our calculations we have used the finite-system version of the DMRG algorithm designed to perform accurate studies for finite size systems [35]. For more details see Ref. [36].

Calculations were performed for films of width L between 100 and 200 at the bulk critical temperature $T=T_c$, and for surface fields $H_1=H_L$ ranging from $H_1=10^{-7}$ to 10. The magnetization profiles obtained from the exact and approximate methods show remarkable agreement with a precision of about one part in 10^6 or better. A selection of profiles calculated for the film of width $L=200$ at $T=T_c$ is shown in Fig. 1(a). We can distinguish three different regimes of H_1 (a) strong H_1, for which $L/l_1 \gg 1$, (b) intermediate H_1 [$L/l_1=O(1)$], and (c) very weak H_1, for which $L/l_1 \ll 1$.

(a) *Strong surface field (microscopic l_1).* For the strongest surface fields, H_1 between ten and approximately 0.5, the profiles take the familiar $y=\infty$ fixed point shape, i.e., they decrease monotonically towards the center of the film. In this regime of H_1 the length l_1 lies between $l_1(H_1=10) \approx 0.009(1)$ and $l_1(H_1=0.6)\approx 2.5(3)$. As H_1 is reduced from 10 to 0.6, the surface layer magnetization m_1 decreases rapidly, whereas the magnetization in the central part of the film remains almost the same (see Fig. 2). As a consequence, the adsorption Γ also changes, although the H_1 dependence in this regime is very weak. For $H_1\approx 0.4$, Γ starts to saturate at a value which depends on the size of the system L. According to the critical point finite-size scaling predictions of Eq. (2.18), $\Gamma \sim L^{-7/8}$ for large H_1. In Fig. 3 we show logarithmic plot of the critical-point scaling function $\mathcal{G}_c(xy)$ [see Eq. (2.18)] of the adsorption Γ. For the scaling variable $xy \sim L/l_1 = LH_1^2 \approx 20\,000$ in two dimensions the magnetization profile is almost saturated, and coincides very well with the exact profile (2.20) of the limiting case $xy\to\infty$. We can estimate, that for this value of xy, $\mathcal{G}_c(xy)$ achieves its asymptotic fixed point value.

(b) *Intermediate surface field* ($1<l_1\leqslant L$). The shapes of the profiles change qualitatively for $H_1\leqslant 0.5$. Now the length l_1 is equal to a few lattice spacings and, in agreement with the behavior found for the semi-infinite systems (see Sec. II A), the maximum order is shifted away from the walls. Two symmetric maxima appear at $z\sim l_1$ and $z\sim L-l_1$—see Fig. 1. As H_1 is lowered further, the maxima become flat and extended and they move towards the center of the film. The surface magnetization still decreases fairly rapidly with decreasing H_1, whereas the value of the magnetization at the center changes only very slightly and for $H_1=0.2$ it is already higher than m_1 (see Fig. 2). For $l_1\approx L$, i.e., $H_1 \approx 0.07$, the two separate maxima in m_l merge into one located at the center of the film and the profiles *increase* monotonically toward the center of the film. In this range of surface fields the maximum order (the maximum magnetization) crosses over from the surface to the center of the film, as is shown in Fig. 2. The coverage Γ also crosses over from

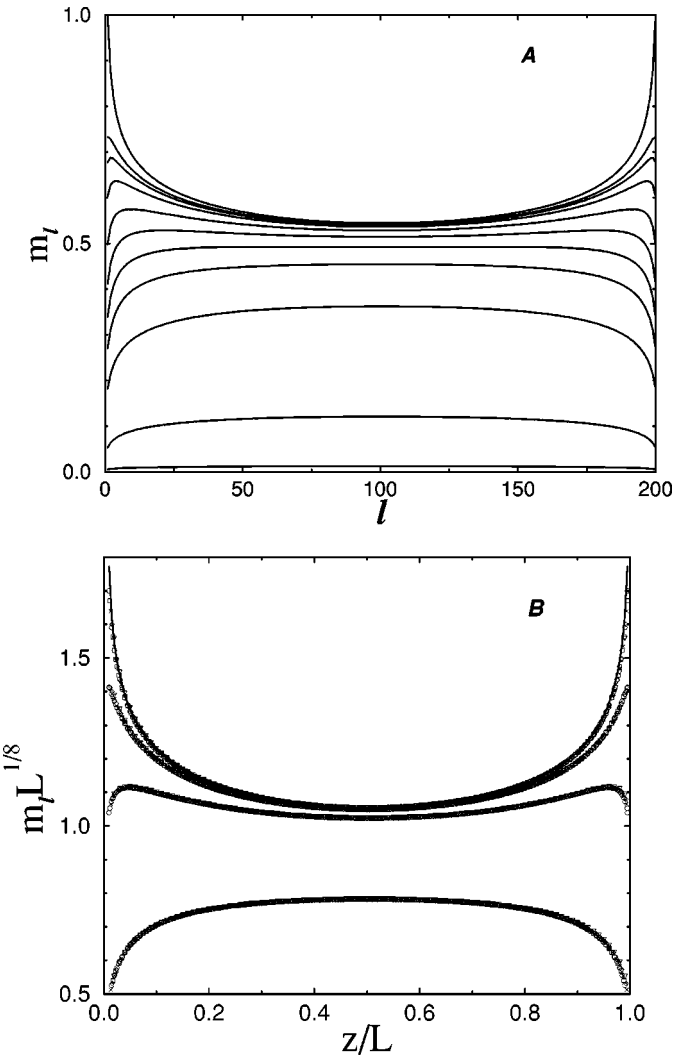

FIG. 1. (a) Magnetization profiles m_l for the 2D Ising film of width $L=200$ at zero bulk field and several values of the surface field $H_1=H_L$: the top profile corresponds to $H_1=10$, then subsequently from the next to the top to the bottom profile: $H_1=0.5$, 0.4, 0.3, 0.2, 0.14, 0.1, 0.07, 0.04, 0.01, and 0.001. (b) Scaling functions of typical magnetization profiles in three regimes of the surface field H_1 (see Sec. III) corresponding to the scaling variable $xy=LH_1^2$. From top to bottom, $xy=20\,000$ and 50—strong H_1 regime; $xy=8$—intermediate H_1 regime; and $xy=0.5$—very weak H_1 regime. The solid-line curve is the scaling function of the profile at the fixed point $xy=\infty$ [Eq. (2.20)].

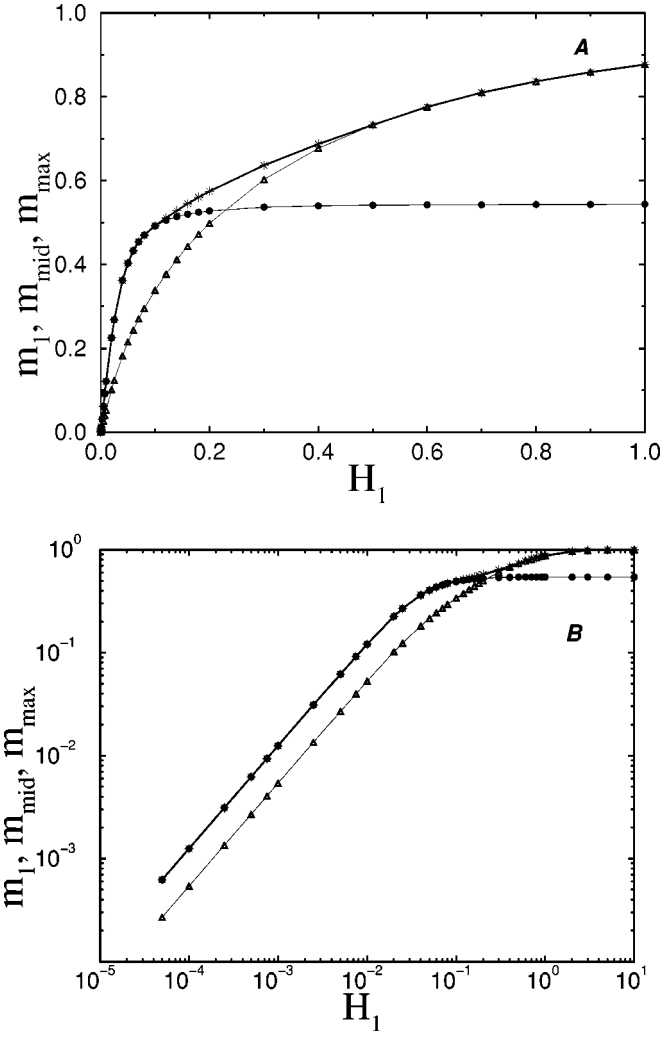

FIG. 2. (a) Surface magnetization m_1 (triangles), magnetization in the center of the film m_{mid} (circles), and the maximum value of the magnetization in the whole film $m_{\max}$ (stars) for the critical ($T=T_c$) 2D Ising film of width $L=200$, plotted as a function of H_1. The maximum value of the order parameter crosses over from being at the surface to being at the middle of the system as the surface field becomes weaker. (b) The same results as in (a) but now plotted on a logarithmic scale to expose the linear dependence of the OP on H_1 for very weak surface fields.

being almost constant to being a rapidly decreasing function of decreasing H_1 (see Fig. 3).

(c) *Weak and vanishing surface field* ($l_1 \gg L$). For very weak surface fields, corresponding to $L/l_1 \ll 1$, profiles increase monotonically toward the center of the film, but now the value of the magnetization both at the surface and in the middle of the film rapidly goes to zero with H_1. For $H_1 \approx 0.01$ and below it is seen from the log-log plot [Fig. 2(b)] that *both* m_1 and m_{mid} decrease linearly with H_1. The linear dependence of m_1 on H_1 for weak surface field in the 2D Ising strip is a known result [32], but more careful inspection of our results shows that there is a logarithmic correction to this linear dependence for l_1 greater than L, i.e., $m_1, m_{\mathrm{mid}} \sim H_1 \ln H_1$. This logarithmic factor can be traced back to the logarithmic singularity of the surface susceptibility. Moreover, we find that in fact the *whole* profile depends linearly (up to the logarithmic factor) on H_1 when l_1 becomes greater

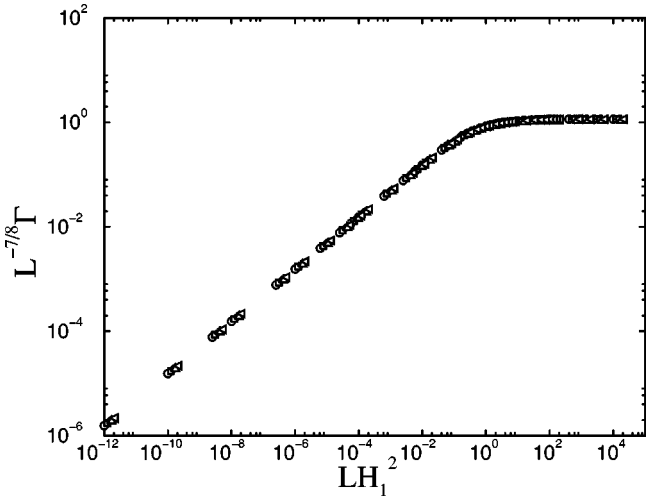

FIG. 3. Log-log plot of the scaling function $\mathcal{G}_c(xy)$ [obtained using Eq. (2.18)] of the adsorption Γ calculated for the critical ($T=T_c$) 2D Ising films of different widths L between 100 and 200. On the logarithmic scale, $\mathcal{G}_c(xy)$ forms a straight line with a slope equal to 1/2 for $xy<0.03$.

than L. This result agrees (up to the logarithmic factor specific for the 2D Ising model) with the physical interpretation of the length l_1 (see Sec. I) as the approximate distance from the surface up to which the OP responds linearly to the surface field H_1; now l_1 is greater than L, so that the whole system responds linearly to H_1.

The coverage Γ also decreases rapidly to zero. A linear dependence of the whole profile on H_1 (up to the logarithmic factor) implies the same dependence of Γ on H_1. The linear factor can be deduced from a logarithmic plot of the scaling function of Γ (Fig. 3), which shows the scaling function $\mathcal{G}_c(xy=LH_1^2)$ decaying according to a power law for $xy<0.03$ with an exponent equal to $\Delta_1/\nu=1/2$. The linear behavior of Γ for weak surface fields was assumed in Ref. [37], and is consistent with the measurements of the surface tension for typical liquid binary mixtures near the critical endpoint. The L dependence of the adsorption in this regime of the surface fields follows immediately from the scaling form of Γ [Eq. (2.18)], i.e., $\Gamma \sim L^{(\nu-\beta)/\nu}(LH_1^{\nu/\Delta_1})^{\Delta_1/\nu} = L^{(\nu-\beta+\Delta_1)/\nu} = L^{11/8}$ in 2D Ising systems.

In Fig. 1(b) we present scaling functions as defined by Eq. (2.17) of typical profiles corresponding to the scaling variable $xy=0.5$, 8, 50, and 20 000 together with the scaling function of the profile at fixed point $xy=\infty$, given by Eq. (2.20). The scaling of the profiles calculated for widths of the film from $L=100$ to 200 is excellent. For all the values of xy the curves collapse onto each other with very high accuracy, confirming that the scaling dominant L dependence for the profiles is $L^{-\beta/\nu}$. We have checked that for $xy=20\,000$ the profile is almost saturated, and mimics the limiting case $xy \to \infty$. Therefore we could use it to fix the scaling constant $\mathcal{A}$ in Eq. (2.20), equating the values of both profiles in the middle of the strip. Because in the limit $xy \to \infty$ our first ($L=1$) and last ($L=200$) columns become the walls of fixed spins, in order to obtain appropriate profiles we put $L=199$ in the exact formula (2.20), corresponding to 198 unfixed spins.

To assess the accuracy of the DMRG method, we calcu-

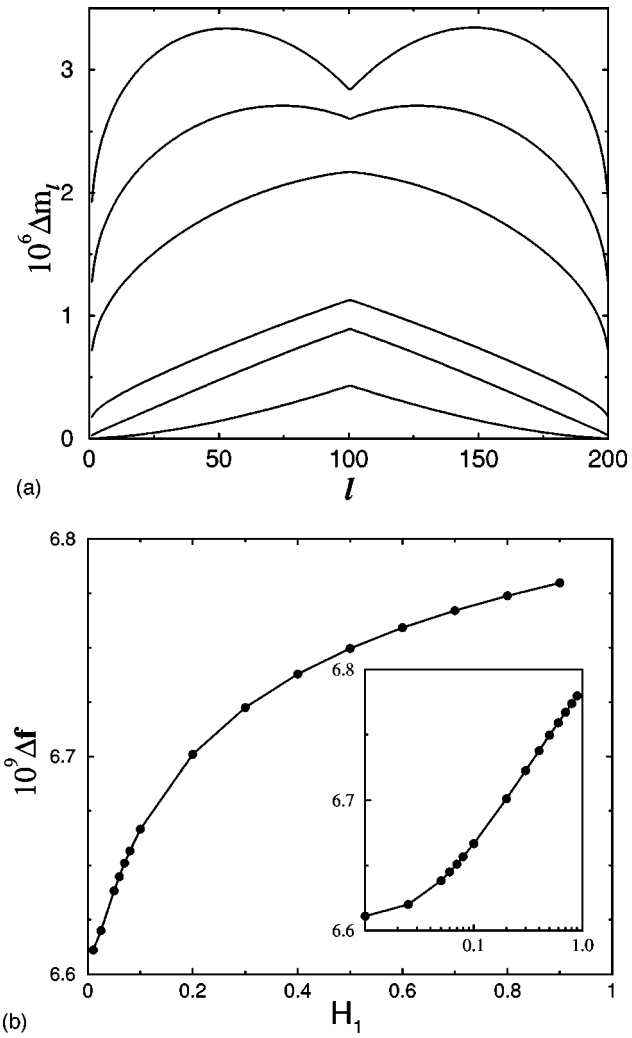

FIG. 4. (a) Reduced errors of the DMRG profiles [see Eq. (3.1)]. Surface fields H_1 from the bottom to the top are $H_1=0.8$, 0.5, 0.1, 0.07, 0.04, and 0.01. For $H_1<0.08$ the error decreases approximately linearly with the surface field. The values of errors have been multiplied by 10^6. (b) Reduced errors of the DMRG free energy per spin [see Eq. (4.10)]. Inset: semilog plot of the same curve to expose the logarithmic behavior of errors for larger H_1. The values of errors have been multiplied by 10^9.

late the relative difference between the profiles obtained using the DMRG and the exact diagonalization methods,

$$(m_l^{\mathrm{DMRG}}-m_l^{\mathrm{exTM}})/m_l^{\mathrm{exTM}}, \tag{3.1}$$

for a few choices of H_1 corresponding to the three different regimes of the surface fields as described above. The accuracy of the DMRG method changes with the value of H_1 [see Fig. 4(a)]. Generally, the larger the fluctuations of spins are in the system, the larger the relative errors. The accuracy is best in the regime (a)- for the strongest fields. As the value of H_1 decreases, the system approaches bulk criticality and accuracy decreases. DMRG calculations for a film of width $L=200$ and $m=32$ states kept fixed in each iteration give a relative difference in Eq. (3.1) that is smaller than 10^{-6} for $H_1>0.1$ (l_1 approximately less than 90). When the surface field decreases to $H_1=0.01$ ($l_1\sim 9090$) the error is around 3×10^{-6}.

It turns out that accuracy of the DMRG calculations depends on the distance from the surfaces in a way that is related to the fluctuations. In regime (a) the system is most strongly ordered near the surfaces and, accordingly, the error is smallest there and has a maximum in the middle of the film. When H_1 enters the regime of very weak surface fields the region of highest order shifts to the middle of the film and the accuracy is best there [see Fig. 4(a)].

IV. RESULTS FOR THE SOLVATION FORCE

In the transfer-matrix approach the leading eigenvalue λ_L of the transfer matrix T_L,

$$T_L|v_L\rangle=\lambda_L|v_L\rangle, \tag{4.1}$$

gives the free energy per spin of an Ising film as

$$\beta f_L=-\frac{1}{L}\ln\lambda_L. \tag{4.2}$$

The exact diagonalization for the 2D Ising film with surface fields $H_1=H_L$ gives [34]

$$\lambda_L=\exp\left(\frac{1}{2}\sum_{i=0}^{L}\gamma(\omega_i)\right), \tag{4.3}$$

$$\cosh\gamma=\cosh(v_2-v_1)+1-\cos\omega, \tag{4.4}$$

where $v_2=2K$, $v_1=2K^*$, $K=\beta J$, $\beta=1/k_BT$, and the relation $\sinh 2K^*\sinh 2K=1$ defines $K^*(K)$. The angles ω_i are obtained from a certain transcendental equation which depends on temperature. The case $T=T_c$ was not considered in Ref. [34], so we discuss it briefly below. At the bulk critical temperature $v_1=v_2\equiv v_c=\ln(1+\sqrt{2})$ and ω_k are L numbers between 0 and π which are roots of the equation

$$\tan L\omega=\tan(\delta'+\phi)(\omega), \tag{4.5}$$

$$(\delta'+\phi)(\omega)=M\omega-(k-1)\pi, \tag{4.6}$$

where

$$e^{i\delta'(\omega)}=e^{-v_c}\left(\frac{e^{i\omega}-e^{2v_c}}{e^{i\omega}-e^{-2v_c}}\right)^{1/2}, \tag{4.7}$$

with the square roots being positive for $e^{i\omega}=-1$ and

$$e^{i\phi(\omega)}=i\frac{We^{i\omega}(e^{i\omega}-W^{-1})}{e^{i\omega}-W}, \tag{4.8}$$

where

$$W=(\cosh v_c+1)(\cosh v_c-\cosh 2H_1). \tag{4.9}$$

$\delta'(\omega)$ decreases monotonically from $\pi/2$ at $\omega=0$ to 0 at $\omega=\pi$, whereas $\phi(\omega)$ has a maximum between $\omega=0$ and $\omega=\pi$, and $\phi(0)=\phi(\pi)=\pi$. Examination of Eq. (4.5) shows that all $k=1,\ldots,L$ roots of Eq. (4.5) are real. They can be calculated numerically but to machine accuracy. After inverting of Eq. (4.4) one obtains the quantities γ_k, k

$=1,\ldots,L$ and hence the free energy per spin. In the DMRG method the leading eigenvalue of the *effective* transfer matrix is calculated numerically.

We use both methods to calculate the free energy per spin for various surface fields and widths of the film between 100 and 200. We find that in the case $L=200$ the difference between free energies per spin,

$$(f_{\mathrm{DMRG}}-f_{\mathrm{exact}})/f_{\mathrm{exact}}, \tag{4.10}$$

is a smooth curve as a function of H_1 with values smaller than 7×10^{-9}. The error decreases, when the surface field goes down [see Fig. 4(b)]. Of course, keeping more states ($m=32$ here) would improve the accuracy, but the significant increase of calculation time has kept us from doing it.

In order to find the solvation force at $T=T_c$ we first calculate the excess free energy per unit area $f^{\mathrm{ex}}(L)\equiv[f(L)-f_b]L$ [see Eq. (2.21)], where $f(L)$ is the free energy per spin for the whole system and f_b is the bulk free energy per spin. $f(L)$ is calculated from the leading eigenvalue of the effective transfer matrix [Eq. (4.2)], whereas f_b is known exactly for the 2D Ising model at $T=T_c$ and zero bulk field [38] and its numerical value is approximately equal to $f_b\sim-2.109\,651\,1$. Having values $f^{\mathrm{ex}}(L_0+2)$ and $f^{\mathrm{ex}}(L_0)$, we approximate the derivative in Eq. (2.22) by a finite difference

$$f_{\mathrm{solv}}=-(1/2)[f^{\mathrm{ex}}(L_0+2)-f^{\mathrm{ex}}(L_0)]. \tag{4.11}$$

We estimate that the difference between f_{solv} calculated using the two approaches is of the order of 10^{-7}.

As another test of the DMRG method, we also calculate the bulk free energy at T_c. Keeping $m=48$ states we perform calculations of the free energy for films with widths up to $L=300$. Next we extrapolate the bulk free energy using a powerful extrapolation technique [39] and for $L\to\infty$ we obtain the value f_b with the accuracy 10^{-10}.

We calculate f_{solv} as a function of H_1 for $L=100$, 124, 150, 174, and 200. The solvation force is attractive for all values of H_1 we studied. For a given L, f_{solv} approaches the (same) constant value for $H_1\to\infty$ and $H_1\to0$, but between these two values f_{solv} exhibits a sharp maximum located at a small (less than 0.1), L-dependent value of H_1. Figure 5 presents this most interesting part of the crossover regime. The absolute value of the solvation force at the maximum is approximately *one order of magnitude less* than at $H_1\to\infty,0$. For example, for $L=100$, $f_{\mathrm{solv}}(H_1=10)\approx-1.46\times10^{-5}$, whereas $f_{\mathrm{solv}}^{\mathrm{max}}(H_1\sim0.1)\approx-1.83\times10^{-6}$.

In Fig. 6 we plot $L^2\times|f_{\mathrm{solv}}|$ as a function of the scaling variable $xy=LH_1^2\sim L/l_1$. We obtain an excellent scaling, so we can conclude that the logarithmic part of to the scaling function $\mathcal{F}_2$ [see Eq. (2.28)] vanishes at T_c. This agrees with the results for the scaling function at T_c obtained by Evans and Stecki [14] in the special case of $H_1=H_L=\pm\infty$. As $xy\to0$ and $xy\to\infty$ the scaling function $\mathcal{F}_c(xy)/k_BT_c$ [see Eq. (2.27)] approaches a constant value which, to good accuracy, is equal to $-\pi/48$—the critical Casimir amplitude $A_{1,L}(H_1=H_2=\pm\infty,0)$. The minimum of $|\mathcal{F}_c|$ is reached for the scaling variable $xy_{\mathrm{min}}\approx0.9$, i.e., when l_1 becomes approximately equal to $L(L/l_1\approx1)$.

From the form of the scaling function we can draw conclusions about the behavior of the solvation force for various strength of the confining walls, that is, for various L/l_1. The universal, H_1-independent behavior occurs for $l_1\to0$ and $l_1\to\infty$. For our 2D system the two constant wings of the scaling function correspond to $l_1<10^{-3}L_m$ and to $l_1>10^{3}L_m$, where by L_m we denote the largest wall separation for which the solvation force is measurable. In practice $L_m<10^3$. In the first case H_1 is very strong and the shape of the OP is quantitatively independent of H_1, the boundary layer is saturated, and its magnetization is $m_1=1$. For the second case of very weak or vanishing H_1 the OP profile vanishes in the whole slit. In these two cases the solvation force decreases according to the universal power law (2.24). Between the two extreme cases of very strong and very weak H_1 two qualitatively different behaviors of the solvation force can be observed. The first is for $1<L/l_1<10^2$ and the second is for $10^{-2}<L/l_1<1$.

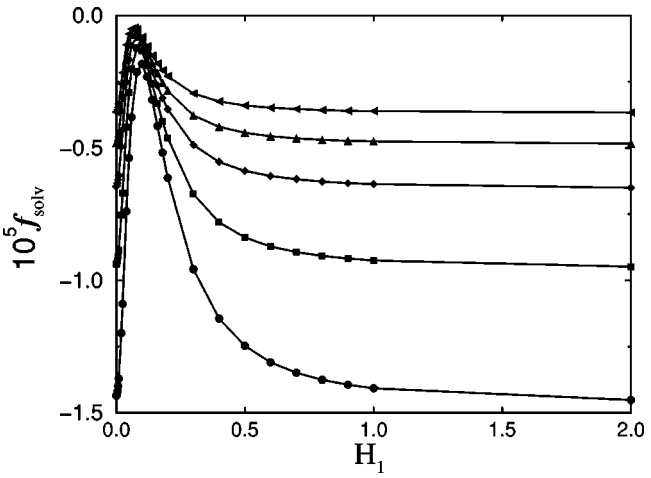

FIG. 5. The solvation force (in units of k_BT) calculated for critical 2D Ising films of widths $L=100$ (circles), 124 (squares), 150 (diamonds), 174 (triangles), and 200 (left closed triangles) as a function of the surface field H_1. The values of the solvation force have been multiplied by 10^5.

(a) $1<L/l_1<10^2$. The decay of the solvation force is *slower* than in the universal regime. This slower decay of the solvation force is associated with the OP profile having two maxima at some distance from the boundary layers.

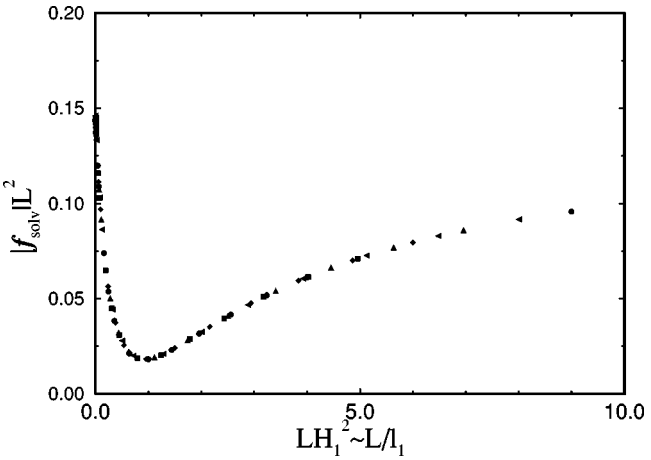

FIG. 6. The modulus of the scaling function of the solvation force $\mathcal{F}_c$ [Eq. (2.27)] calculated for 2D Ising films of widths between 100 and 200.

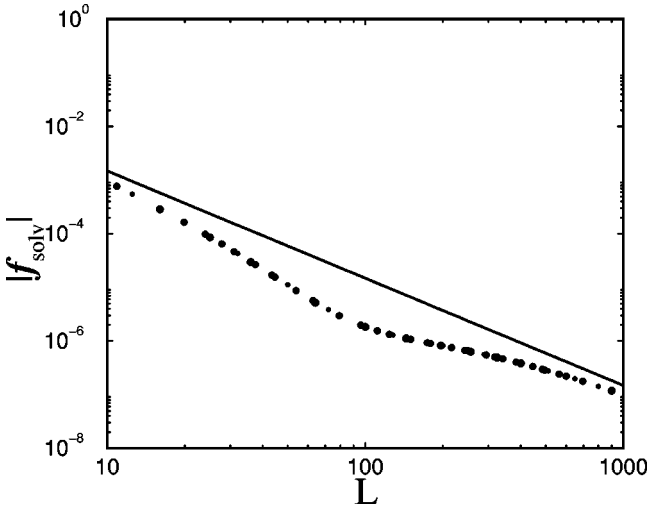

FIG. 7. Log-log plot of the modulus of the solvation force as a function of the width L for 2D Ising films subject to weak surface fields $H_1=H_L=0.1$. The solid line shows the universal fixed point decay $-\pi/(48k_BT_c)L^{-2}$.

(b) $10^{-2}<L/l_1<1$. In this regime the decay of the solvation force is *faster* than in the universal regime. The faster decay of the solvation force is associated with the OP profile depending linearly on H_1, and having a single maximum in the center of the film.

For the particular choice of the surface field, i.e., for $H_1=0.1$, the universal power-law decay of the solvation force cannot take place in a measurable range of widths of the film as shown in Fig. 7. Around the minimum of the absolute value of the scaling function in Fig. 6, i.e., for the scaling argument between 0.3 and 3, we fit $\mathcal{F}_c$ to a polynomial of the tenth degree. From the fit we obtain the behavior of the solvation force close to the minimum. Figure 8 shows this behavior for particular choice of the surface field $H_1=0.1$. For $100<L<300$ the solvation force is almost independent of L.

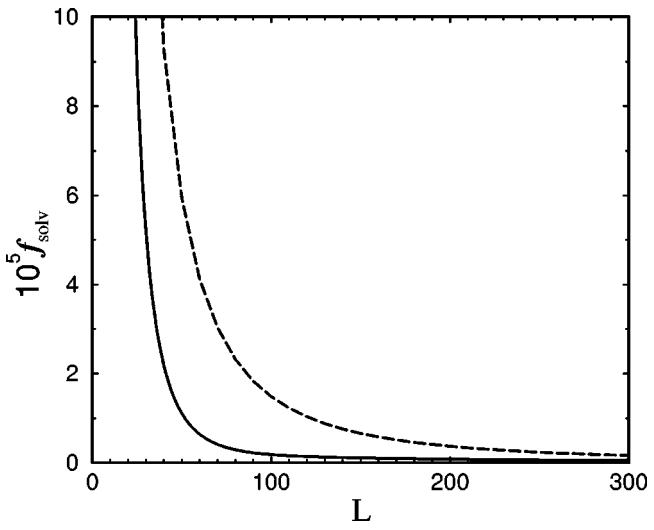

FIG. 8. The modulus of the solvation force (multiplied by 10^5) for weak surface fields $H_1=H_L=0.1$ obtained from the fit of the scaling function to a polynomial of the 10th degree. The fit is valid for $30<L<300$. The long-dashed line shows the universal fixed-point decay $-\pi/(48k_BT_c)L^{-2}$.

V. SUMMARY AND CONCLUSIONS

We have studied how the magnetization profiles, the adsorption (the excess magnetization) and the ''magnetic'' solvation force of 2D Ising films change at bulk criticality as the surface fields $H_1=H_L$ are varied between 0 and ∞. Our predictions that nonuniversal properties of critical phenomena in the crossover regime should manifest themselves particularly strongly in the confined systems have been fully confirmed.

The scaling functions of all the calculated quantities deviate substantially from their asymptotic forms at the fixed points over a wide range of H_1 and L. This may be relevant for experiments. The solvation force as a function of L, $f_{solv}(L)$, should depend on a particular choice of confining walls for which H_1 is usually fixed. We predict that universal decay of $f_{solv}(L)$, through the whole range of wall separations $L>1$, can be found only for very strong surface fields such that $l_1<10^{-2}$. For weaker H_1 ($10^{-2}<l_1<1$) the solvation force should decay in a slower fashion for $1<L<10^2 l_1$, and for larger wall separations the crossover to a universal behavior should take place. The most interesting behavior is predicted for weak surface fields ($1<l_1<10^2$). Then, for $1<L<l_1$ the solvation force should decay *faster* than at the fixed points, and for larger wall separations a crossover to decay *slower* than L^{-d} should occur. For still larger wall separations, $L>10^2 l_1$, another crossover to the universal decay law should occur (in practice the solvation force is not measurable for distances which are as large as this). Finally, for even weaker H_1 ($l_1>10^2$) the universal decay should be first observed for $1<L<10^{-2}l_1$, and for larger wall separations the crossover to the *faster* decay should occur. Again, a second crossover to the slower decay should be found for $L>l_1$ (this second crossover may not be measurable in practice). The third crossover to the power law L^{-d} occurs for very large wall separations, $L>10^2 l_1>10^4$, and we expect that this behavior is not measurable experimentally.

From the behavior of the solvation force one can draw conclusions about the shape of the OP, since the faster decay is associated with a single maximum in the center of the film, and the slower decay is associated with two maxima, each in the neighborhood of each wall. Moreover, measurements of the solvation force can provide experimental estimate for the strength of the surface field H_1, which cannot be measured directly and, to our knowledge, by no other method. By measuring the decay of the solvation force and knowing L one can estimate, up to the amplitude A_1, the strength of H_1 on the basis of the discussion described above, that is by comparing $l_1 \sim H_1^{-\nu/\Delta_1}$ and L (in dimensionless units).

Our results should be applicable to various systems in the Ising universality class such as magnets, simple fluids, binary alloys, and binary mixtures with short-ranged wall potentials. We expect a qualitatively similar scenario for the crossover between the ordinary and normal transitions in three-dimensional confined systems of analogous geometry. It is not obvious how this crossover manifests itself in the systems with long-ranged wall potentials. In recent simulations of a Lennard-Jones fluid in a 3D slit with long-ranged wall potentials, the critical OP profiles showed features similar to those we obtained for the weak field H_1, provided the amplitude of the attractive wall potentials was small [40].

These amplitudes may correspond to walls, weakly favoring one of the phases, but more systematic studies are needed.

Our predictions concerning the explicit dependence of measurable quantities, such as the adsorption and the solvation force, on the strength of the surface field H_1 could be verified experimentally. For example, in the experiments on binary mixtures [8] in semi-infinite geometry the walls of the container changed their preference from one component to another as a function of time, the time scale of this change being of the order of days, so that the average surface field H_1 during certain days was small. Such walls could be used for studying the confined system.

Encouraged by the very good accuracy of the DMRG method at the bulk critical temperature and zero bulk field, as determined by comparing with the exact results, we are currently using this method to study the same system away from the critical point, including nonzero bulk field. From our analysis of the errors it follows that the accuracy of this method should be even better away from the critical point.

ACKNOWLEDGMENTS

A.M. benefited from discussions with R. Evans, P. Upton, and J. O. Indekeu. She also thanks the Royal Society/NATO for financial support. A.D. would like to thank Professor D. Bollé and the Institute for Theoretical Physics of the Catholic University of Leuven for providing computer facilities on which part of the calculations were performed, and Maciej Dudziński for several discussions. We are grateful to R. Evans for a critical reading of the manuscript. This work was partially funded by KBN Grant Nos. 2P03B10616 and 3T09A07316.

[1] K. Binder, *Phase Transitions and Critical Phenomena* edited by C. Domb and J. L. Lebowitz (Academic Press, London, 1983), Vol. 8, p. 1.
[2] H. Diehl, *Phase Transitions and Critical Phenomena*, edited by C. Domb and J. L. Lebowitz (Academic Press, London, 1986), Vol. 10, p. 75.
[3] H. Dosch, *Critical Phenomena at Surfaces and Interfaces*, edited by G. Höhler and E. A. Niekisch (Springer, Berlin, 1992), Vol. 126, p. 1.
[4] H. Diehl, Int. J. Mod. Phys. B **11**, 3593 (1997).
[5] U. Ritschel and P. Czerner, Phys. Rev. Lett. **77**, 3645 (1996) and references therein.
[6] A. Ciach and U. Ritschel, Nucl. Phys. B **489**, 653 (1997).
[7] A. Ciach, A. Maciołek, and J. Stecki, J. Chem. Phys. **108**, 5913 (1997).
[8] N. S. Desai, S. Peach, and C. Franck, Phys. Rev. E **52**, 4129 (1995).
[9] R. Evans, *Liquids at Interfaces* in Les Houches Session XLVIII (Elsevier, Amsterdam, 1990), p. 3.
[10] J. N. Israelachvili and P. M. McGuggian, Science **241**, 795 (1988).
[11] L. Spruch, Science **272**, 1452 (1996).
[12] M. Krech, in *The Casimir Effect in Critical System* (World Scientific, Singapore, 1994), and references therein.
[13] J. L. Cardy, Nucl. Phys. B **275**, 200 (1986).
[14] R. Evans and J. Stecki, Phys. Rev. B **49**, 8842 (1993).
[15] M. Krech and D. P. Landau, Phys. Rev. E **53**, 4414 (1996).
[16] M. Krech, Phys. Rev. E **56**, 1642 (1997).
[17] M. P. Nightingale and J. O. Indekeu, Phys. Rev. Lett. **55**, 1700 (1985).
[18] J. O. Indekeu, M. P. Nightingale, and W. V. Wang, Phys. Rev. B **34**, 330 (1986).
[19] T. Nishino, J. Phys. Soc. Jpn. **64**, 3598 (1995).
[20] A. Drzewiński, A. Ciach, and A. Maciolek, Eur. Phys. J. B **5**, 825 (1998).
[21] E. Carlon and A. Drzewiński, Phys. Rev. Lett. **79**, 1591 (1997).
[22] E. Carlon, A. Drzewiński, and J. Rogiers, Phys. Rev. B **58**, 5070 (1998).
[23] E. Carlon and F. Igói, Phys. Rev. B **57**, 7877 (1998).
[24] M. E. Fisher and P. de Gennes, C. R. Seances Acad. Sci., Ser. B **287**, 207 (1978).
[25] R. Z. Bariev, Theor. Math. Phys. **77**, 1090 (1988).
[26] R. Konik, A. LeClair, and G. Mussardo, Int. J. Mod. Phys. A **11**, 2075 (1997).
[27] P. Czerner and U. Ritschel, Int. J. Mod. Phys. B **11**, 2765 (1996).
[28] A. M. Ferrenberg and D. P. Landau, Phys. Rev. B **44**, 5081 (1991).
[29] M. N. Barber, in *Phase Transitions and Critical Phenomena*, edited by C. Domb and J. L. Lebowitz (Academic Press, London, 1983), Vol. 8, p. 1.
[30] T. W. Burkhardt and T. Xue, Phys. Rev. Lett. **66**, 895 (1991).
[31] J. Stecki, A. Maciołek, and K. Olaussen, Phys. Rev. B **49**, 1092 (1993).
[32] H. Au-Yang and M. E. Fisher, Phys. Rev. B **21**, 3956 (1980).
[33] V. Privman and M. E. Fisher, Phys. Rev. B **30**, 322 (1984).
[34] A. Maciołek and J. Stecki, Phys. Rev. B **54**, 1128 (1996).
[35] S. R. White, Phys. Rev. B **48**, 10 345 (1993).
[36] *Lectures Notes in Physics*, edited by I. Peschel, X. Wang, M. Kaulke, and K. Hallberg (Springer, New York, 1999), Vol. 528.
[37] W. Fenzl, Europhys. Lett. **24**, 557 (1993).
[38] L. Onsager, Phys. Rev. **65**, 117 (1944).
[39] R. Bulirsch and J. Stoer, Numer. Math. **6**, 413 (1964); M. Henkel and G. Schütz, J. Phys. A **21**, 2617 (1988).
[40] N. B. Wilding (private communication).